Journal of Electron Spectroscopy and Related Phenomena 224 (2018) 38–44

Contents lists available at ScienceDirect

Journal of Electron Spectroscopy and Related Phenomena

journal homepage: www.elsevier.com/locate/elspec

Polarization-dependent resonant inelastic X-ray scattering study at the Cu *L* and O *K*-edges of $YBa_2Cu_3O_{7-x}$

Martin Magnuson [a,*], Thorsten Schmitt [b], Laurent-C. Duda [c]

[a] Department of Physics, Chemistry and Biology, IFM, Thin Film Physics Division, Linköping University, SE-58183, Linköping, Sweden
[b] Research Department Synchrotron Radiation and Nanotechnology, Paul Scherrer Institut, Swiss Light Source (SLS), CH-5232, Villigen PSI, Switzerland
[c] Department of Physics and Astronomy, Division of Molecular and Condensed Matter Physics, Uppsala University, Box 516, S-751 20, Uppsala, Sweden

ARTICLE INFO

Article history:
Received 1 November 2016
Received in revised form 8 July 2017
Accepted 15 July 2017
Available online 19 July 2017

ABSTRACT

We present a study on the high-Tc superconductor (HTSC) $YBa_2Cu_3O_{7-x}$ (YBCO) using polarization-dependent X-ray absorption and resonant inelastic X-ray scattering. High-resolution measurements using synchrotron-radiation are compared with calculations using a quasi-atomic multiplet approach performed at the Cu $2p_{3/2}$-edge of YBCO. We use a multiplet approach within the single impurity Anderson model to reproduce and understand the character of the localized low-energy excitations in YBCO. We observe a distinct peak at about 0.5 eV in O *K* RIXS. This peak shows dependence on doping, incident energy, and momentum transfer that suggests that it has a different origin than the previously discussed cuprate bimagnons. Therefore, we assign it to bimagnon excitations within the Zhang Rice bands and/or the Upper Hubbard bands, respectively.

1. Introduction

$YBa_2Cu_3O_{7-x}$ (YBCO) is one of the archetypical high T_c-superconductors (HTSC) with a transition temperature (T_c = 90.5 K) above the nitrogen boiling point. This is an immense advantage since it makes it easier and more cost effective to cool below its T_c, which is a requirement for being able to reap the benefits of using HTSC in technological applications [1]. Naturally, it would be even better if room temperature HTSC could be found. The path to this goal is, however, hampered by the lack of fundamental understanding what drives the metal-superconductor transition (MST) in the first place. Conventional superconductors are driven by the phonon coupling between the charge carriers in the material and the strength of this coupling sets an upper limit to the attainable transition temperature. Intriguingly, HTSCs possess transition temperatures far above the conventional limit within the Bardeen-Cooper-Schrieffer (BCS) theory [2]. Thus the mechanism for high T_c-superconductivity remains one of the most nagging problems to be solved in correlated electron physics.

YBCO consists of planes of edge-sharing CuO_2 square plaquettes separated by layers containing rare-earth metals and oxygen. YBCO is a unique case for a superconducting cuprate because the *planes* of corner-sharing CuO_2 plaquettes are separated by apical oxygens from a different type of layer that consists of one dimensional CuO_3 *chains*. Generally, the advantage of cuprates is that they are not stoichiometry-restricted. It is possible to continuously tune their carrier concentration from the underdoped region to the overdoped region via the optimally doped compound either by reducing, resp. increasing, oxygen concentration or by metal ion substitution. The orthorhombic structure of doped YBCO consists of CuO_5 pyramids that are elongated along the height (*c*-axis) as a result of Jahn-Teller lattice distortion and electron correlation effects. A *d*-hole in each Cu^{2+} ion occupies the d_{x2-y2} orbital, where the *z*-axis is along the *c*-axis of the crystal. The strong electron correlation effects create localized spins around the Cu sites while the doping and shortening of the *c*-axis leads to the coexistence of the Zhang-Rice spin-singlet. The Cu atoms in the CuO_2 planes are bonded to both O atoms in-plane and with apical O. The Cu d_{x2-y2} is the highest occupied orbital of the CuO_2 planes.

When the hole-concentration *x* increases through excess of oxygen in the chains, an opposite lattice distortion occurs where the Jahn-Teller elongated CuO_5 pyramids contract along the *c*-axis so that the Cu-apical O distance becomes smaller. The effect of doping thus counteracts the effect of lengthening the *c*-axis by the Jahn-Teller distortion. The balanced equilibrium *c*-axis length caused by the combination of electron correlations and doping, play an important role for the orbitals and multiplets. When a dopant hole is introduced in the valence band of cuprates, it also gives rise to a

* Corresponding author.
E-mail address: Martin.Magnuson@ifm.liu.se (M. Magnuson).

https://doi.org/10.1016/j.elspec.2017.07.005
0368-2048/

superposition of singlet hole doped O *2p*-σ orbitals surrounding a Cu dx^2-y^2 singlet state forming a localized Zhang-Rice singlet (ZRS) [3] state in the upper Hubbard band of the CuO_2 planes. The ZRS is thus a superposition of local singlet states.

Recently, we have presented results on YBCO [4] revealing temperature dependent *self-doping effects*, which are pivotal for its metal-superconducting transition. Since one-electron band theory does not sufficiently take into account the strong electron correlations in cuprates, we calculated the many-electron states called *multiplets* in the CuO_5 pyramids. We found that the $2p_z$-orbitals of apical oxygen, which hybridize with Cu(1) $3d_{y2-z2}$-orbitals in the chains and with Cu(2,3) $3d_{z2-r2}$-orbitals in the planes, *reconstruct* upon cooling and an *interlayer charge transfer* from the chains to the planes is induced. This shows directly that superconductivity in YBCO is closely linked with and promoted by a self-doping mechanism for providing the planes with the necessary charge density in order to assume an extraordinary high critical temperature T_c. However, the cause for this reconstruction still remains an open question. In the present paper, we focus on the question whether and how this process is accompanied and possibly mediated by any collective modes, such as phonons and magnons.

2. Experimental and theoretical details

2.1. Sample preparation

Thin films of $YBa_2Cu_3O_{6+x}$ (YBCO) were grown by pulsed laser deposition on (100) $SrTiO_3$ $5 \times 5 \times 0.5$ mm^3 single crystal substrates using 25 nm thick CeO_2 buffer layers deposited using RF sputtering at a temperature of 780 °C as described elsewhere [4]. The layers were deposited with an RF source power of 100 W in a mixed argon-oxygen atmosphere (60% O_2 + 40% Ar) at a partial pressure of 0.1 mbar. The distance between the target and the sample was 30 mm. After CeO_2 deposition, the sample was slowly (10 °C/min) cooled down to room temperature under 500 mbar oxygen pressure and was transferred into the PLD chamber without breaking vacuum. During the deposition of YBCO, a substrate was placed directly into the sapphire sample holder and heated by a SiC radiation heater from the back side. The YBCO films were deposited at the temperature of 820 °C. The oxygen pressure during deposition was set to 0.6 mbar, the repetition rate to 10 Hz and the laser energy density at the target 1.25 J/cm^2. The substrate-to-target distance was set to 60 mm. 7500 laser pulses approximately correspond to YBCO thickness of about 350 nm. To obtain optimal doping, the films were post-annealed in-situ at 550 °C at an oxygen pressure of 750 mbar. The optimally doped sample ($x \approx 0.9$) has a critical temperature of T_c = 90.5 K and a very sharp transition with $\Delta T_c \approx 1$ K signifying high quality of the sample.

2.2. X-ray emission and absorption measurements

The X-ray absorption (XAS) and resonant inelastic X-ray scattering (RIXS) measurements were performed at the Advanced Resonant Spectroscopies (ADRESS) beamline [5] at the Swiss Light Source (SLS), Paul Scherrer Institut, Switzerland, using the Super-Advanced X-ray Emission Spectrometer (SAXES) [6,7]. A photon flux of about 10^{13} photons/sec/0.01% bandwidth was focused to a spot size below 5×55 μm^2 vertically and horizontally (VxH). The Cu L_3 edge XAS measurements were made in the bulk-sensitive total fluorescence yield (TFY) mode with an energy resolution better than 100 meV. For the RIXS measurements at the Cu L_3-edge (O *K*-edge), the combined energy resolution was 120 meV (70 meV). To investigate the anisotropy of the electronic structure, linearly polarized X-rays were used at different incidence angles with the electric field vector (**E**) oriented either (nearly) parallel to the *c*-axis (out-of-plane) or parallel to the CuO_2 planes (in-plane) defined by the *a*-axis and the *b*-axis. More details of the measurements and sample preparation is described elsewhere [4].

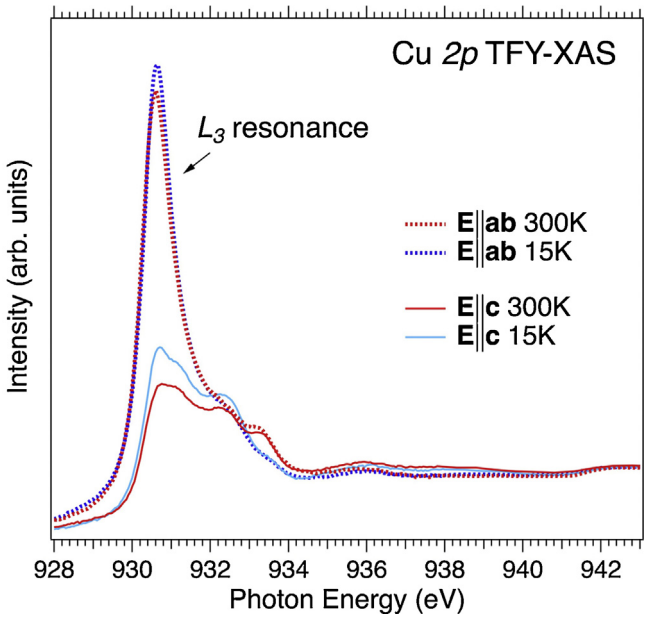

Fig. 1. Polarization- and temperature-dependent X-ray absorption spectra of optimally doped YBCO at the Cu *2p* absorption edge.

2.3. Ligand-field multiplet calculations

The Cu L_3 RIXS spectra of YBCO were calculated in a coherent second-order optical process using the Kramers-Heisenberg formula [8] including interference effects in the intermediate states. The Slater integrals, describing the 3*d*–3*d* and the 3*d*–2*p* Coulomb and exchange interactions, and the spin-orbit splitting were obtained by the Hartree-Fock method [9]. The effect of the configuration-dependent hybridization was taken into account by scaling the Slater integrals to $F_k(3d3d)$ 80%, F_k $(2p3d)$ 80% and G_k $(2p3d)$ 80%. In a crystalline field of octahedral symmetry, the ground state is ^2E_g and in tetrahedral D_{4h} symmetry, this ^2E_g state is further split into the $^2A_{1g}$ and $^2B_{1g}$ states while the $^1A_{1g}$ multiplet is the Zhang-Rice singlet. In D_{4h} symmetry, the ground state of the Cu^{2+} ion has $^2D_{5/2}$ character. We calculated the many-electron ground state (multiplet) for Cu^{2+} ions (Cu $3d^9$) in both D_{4h} and C_4 symmetries.

Due to the Jahn-Teller distortion, the CuO_5 pyramids are elongated, resulting in a longer Cu—O bond (~2.41 Å) along the *c*-axis and four shorter (~1.89 Å) Cu—O bonds in the basal plane. As the Cu electron configurations fluctuate between $3d^{10}$, $3d^9$ and $3d^8$ in the ground state, as in the case of binary transition metal oxides [10] [11], the wave function contains all three configurations in addition to several charge-transfer configurations that were considered.

The single-impurity Anderson model (SIAM) [12] with full multiplet effects was applied to describe the system. The crystal field and exchange interactions were taken into account by using a code by Butler [13] and the charge-transfer effect was implemented with a code [14] developed by Theo Thole. The charge-transfer energy Δ, defined as the energy difference between the center of gravity between the main line and the different charge-transfer configurations, was chosen to reproduce the experiment (Δ_{gs} = 4.1 eV and Δ_{is} = 4.25 eV), and the crystal-field splitting in the $3d^9$ D_{4h} local symmetry was $10Dq$ = 1.5, D_s = 0.3, D_t = 0.16. The three E_{dxy} = −1.50 eV, E_{dxz} and E_{dyz} = −1.60 eV orbitals indicated in Fig. 3 are collectively referred to as t_{2g} and the $E_{dx^2-y^2}$ = 0 and

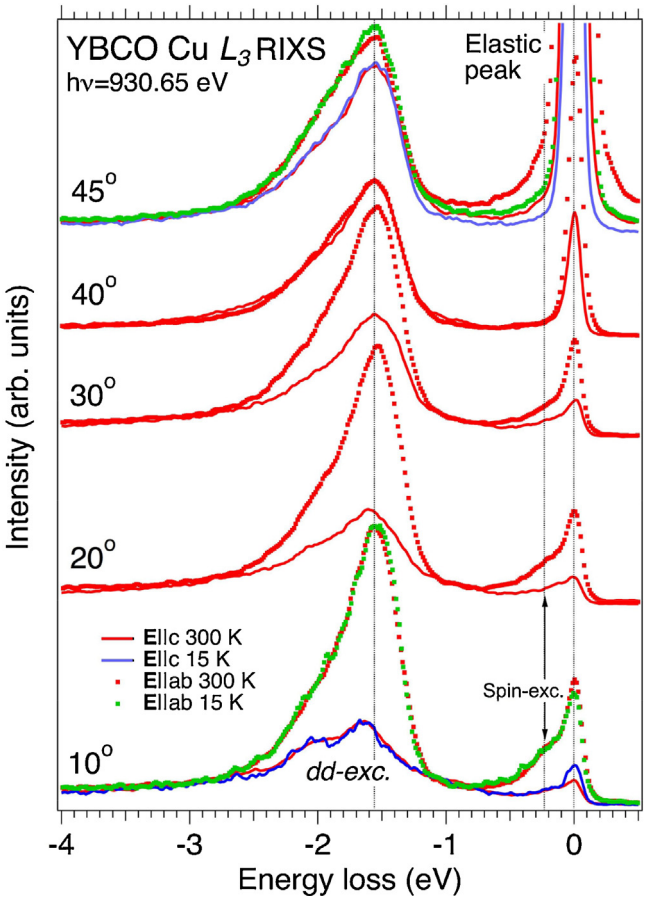

Fig. 2. Angular-dependent Cu L_3-RIXS spectra at 10°, 20°, 30°, 40° and 45° grazing incidence angles with horizontal and vertical polarization for optimally doped YBCO.

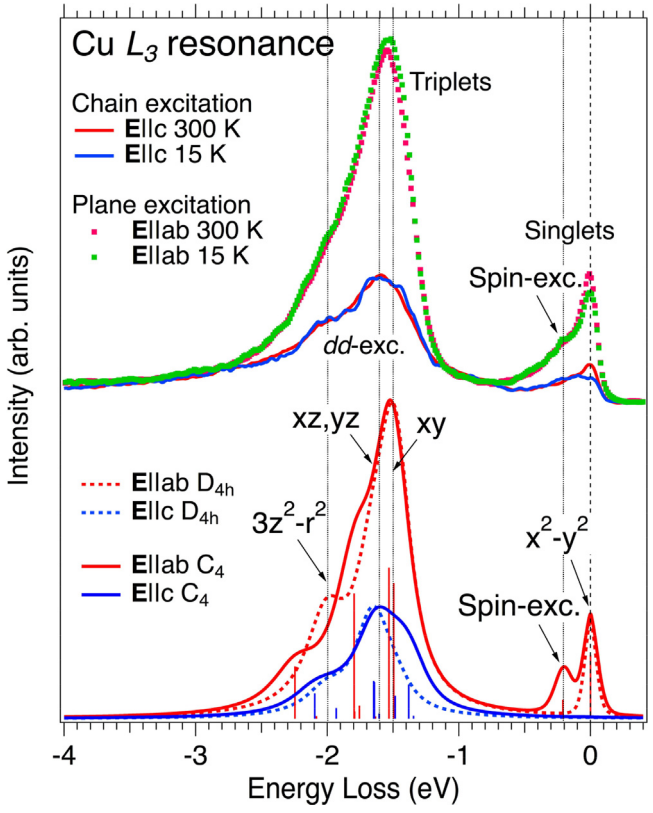

Fig. 3. (top) Cu L_3 resonance RIXS spectra excited at 930.7 eV. Bottom: Calculated spectra with $3d^9$ (Cu^{2+}) final states in D_{4h} and C_4 symmetry including a Cu $3d_{x2\text{-}y2}$ super-exchange energy of 0.21 eV. The vertical blue and red sticks indicate the intensities and energy positions of the transitions to the final states in the calculated RIXS spectra in C_4 symmetry. The three $E_{dxy} = -1.50$ eV, E_{dxz} and $E_{dyz} = -1.60$ eV orbitals collectively referred to as t_{2g} and the $E_{dx2\text{-}y2} = 0$ and $E_{dz2\text{-}r2} = -2.00$ eV orbitals as e_g, are indicated by the vertical dotted lines. (For interpretation of the references to colour in this figure legend, the reader is referred to the web version of this article.)

$E_{dz^2\text{-}r^2} = -2.00$ eV orbitals are referred to as e_g. The calculations were made for the same geometry as the experimental one, with the scattering angle between the incoming and outgoing photons fixed to 90°. The z-axis was perpendicular to the ab plane and the $d_{x2\text{-}y2}$ orbital was in the basal ab-plane. To test the effect of the exchange interaction inducing spin-flip magnon excitations, the calculations were also made in the C_4 basis set with an inter-atomic exchange field of 0.21 eV.

3. Results and discussion

3.1. Cu L-edge XAS

Fig. 1 shows incident angle- and temperature-dependent X-ray absorption spectra of optimally doped YBCO at the Cu $2p$ absorption edge. In particular, we note the peculiar threshold shoulders that are absent in XAS spectra of pure Cu [15]. These shoulders are related to Zhang-Rice [3] plane-, and chain- excitations, respectively. The temperature-dependence of these shoulders has been thoroughly discussed in a previous paper [4]. In this paper, the energy at the main L_3 resonance is used as excitation energy for the L-edge RIXS spectra.

3.2. Cu L-edge RIXS

Fig. 2 shows angular- and temperature-dependent Cu L_3-RIXS spectra of optimally doped YBCO measured at 10°, 20°, 30°, 40° and 45° glancing incidence angles with horizontal and vertical polarization for a scattering angle of 90°. At 45° incidence angle (specular geometry), the elastic peak is very intense, while at the lower angles, it is largely suppressed, in particular, when **E||c**. At 45° incidence angle, the intensity of the dd-excitations is already rather independent of the incident X-ray polarization while at the lower incidence angles, the intensity is very anisotropic with more unoccupied states in-plane than out-of-plane. Note that as the incidence angle is lowered, a shoulder below the elastic peak increases (−0.21 eV), in particular, for the in-plane excitation. This feature can tentatively be assigned to a local spin-flip excitation while collective excitations such as acoustic phonon modes also occur in the mid-infrared region (MIR). Recent momentum dependent Cu L-RIXS results [16] [17] have revealed a considerable dispersion within this energy region that is mainly due to single magnon excitations, although other contributions are not negligible. In RIXS at the Cu L-edge of the $La_{2-x}Sr_xCuO_4$ family [18], of $Bi_2Sr_2CaCu_2O_{8+\delta}$ [19] as well as of $Sr_{14}Cu_{24}O_{41}$ [20] dispersive magnetic modes have been observed at similar energies. Here we will attempt to describe the Cu L-RIXS within a ligand field multiplet model [21] that projects the local contributions.

Fig. 3 shows a close up of the resonant L_3 spectra measured at 20° incidence angle in comparison to calculated model spectra with $3d^9$ (Cu^{2+}) final states in D_{4h} and C_4 symmetries. The C_4 symmetry is applied to include a Cu $3d_{x2\text{-}y2}$ super-exchange energy of 0.21 eV. Within the approximations of multiplet theory, there is no effective difference between the C_{4h} and the C_{4v} symmetries with horizontal and vertical mirror planes, respectively. This means that the crystal field parameters (10Dq, D_s and D_t) for C_4 approximately describe both C_{4v} and C_{4h} symmetries. In undoped $YBa_2Cu_3O_6$, the Cu(1) and Cu(2) atoms in the chains and planes have D_{4h} and C_{4v}symmetries, respecively [22]. Thus, these symmetries are also appoximations of

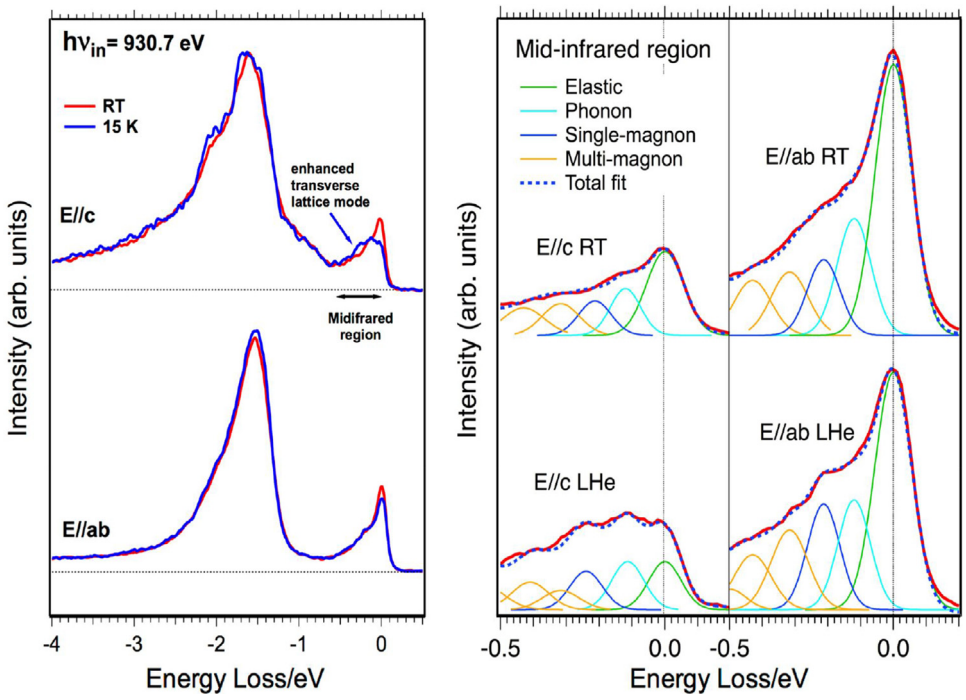

Fig. 4. Mid-infrared energy region of RIXS excited at the Cu L_3 resonance (930.7 eV). The elastic peak appears at 0 eV. Our curve fit helps identify a single phonon mode at 116 meV, a single-magnon mode at 230 meV (246 meV out-of-plane) and multi-magnon modes at 320 meV (mainly in-plane) and 390 meV.

the doped $YBa_2Cu_3O_{7-\delta}$ system, where the Cu(1) and Cu(2) atoms in the chains and planes, respectively, have D_{2h} and C_{2v} symmetries. Excitation close to the L_3 resonance (930.7 eV with 120 meV resolution) yields simulated spectra that are dominated by *dd*-excitations (of $3d^9$-configuration) around −1.5 eV. The Cu^{2+} charge transfer multiplet final state orbital energies were then found to have energies of distorted divalent Cu orbitals in ($E_{dx^2-y^2} = 0$, $E_{dxy} = -1.50$ eV) and perpendicular to ($E_{d3z^2-r^2} = -2.00$ eV) the CuO_2-planes. Based on our observations and experience from reasonable values of distortions in other cuprate systems [16,23], the d_{x2-y2}, d_{xy} and d_{z2} orbital energies and the spin-flip excitation resolved in the RIXS experiment was transferred into crystal field parameters [14] 10Dq, D_s and D_t and the exchange field (0.21 eV). The effect of the exchange field in C_4 symmetry is clearly observed in the presented theoretical spectrum as a spin flip. The general spectral shape of the *dd*-orbital excitations as well as the spin-excitation peak is similar above and below the MST [14,24]. Therefore, the residual temperature dependence in the experimental spectra is ascribed to effects on the collective lattice modes due to the MST. For instance, it is observed that the elastic peak loses intensity by cooling. Upon cooling, the intensity at 0 eV is lowered as the number of holes is increased and the superconducting gap is formed. As the carriers lower their kinetic energy at the MST, the spectral weight is transferred from the E_F and the elastic peak decreases. Recently, Magnuson *et al.* [4] were able to detect that cooling from room temperature to 15 K leads to a significant orbital reconstruction and charge transfer between the CuO_2 planes and the CuO_3-chains. In particular, the involvement of apical oxygen ions in the binding to the Cu ions in the planes and chains makes the temperature dependence of (non-electronic) excitations in the MIR intriguing.

Fig. 4 (left panel) shows the temperature dependence of the resonantly excited Cu L_3 RIXS spectra. The arrow in the top of the left panel points out an enhancement (∼250 meV) that the (**E**//**c**) lattice mode perpendicular to the CuO_2 basal plane acquires at low temperature. The right panel shows a close-up of the MIR for the same spectra. By using a phenomenological multi-Gaussian fit for **E**//**c** (left) and **E**//**ab** polarizations (right), we try to capture the general behaviour instead of the more rigorous approach for instance in Refs. [16,23,25]. This leads to a series of peaks that are narrower than use of the full formalism would yield. Nevertheless, they correspond to visible spectral features, and using the assignments of previous works as guide this allows us to make the following tentative assignments: the elastic peak at 0 eV, a possible single phonon mode at 116 meV (not reported in previous literature), a single-magnon mode at 230–246 meV (higher value out-of-plane) and multi-magnon modes at above 320 meV. This can be compared with similar values of $Sr_2CuO_2Cl_2$, where one-, two, and three-magnon contributions have been predicted around 300–400 meV [26,27]. The higher energy and frequency of the single-magnon mode along the *c*-axis might be related to a longer bond length between the Cu(1)O-chain orbitals compared to the in-plane Cu(2,3)O_2-plane orbitals in the basal *ab*-plane or the same mode that is dressed differently using different polarizations.

We find that sample cooling leads to a strong increase of the single magnon mode (dark blue traces in the left panels of Fig. 4) excited in the basal CuO_2 plane and a decrease of the out-of-plane excited elastic peak (green traces in the left panels of Fig. 4). Note that the phonon modes along the *c*-axis, in particular, show intriguing temperature dependences that will be addressed using future higher-resolving RIXS instrumentation. In addition, optical phonons are hidden in the elastic peak, unresolved in our present RIXS study that could be important for the MST of YBCO. Recently, resonantly driven phonon modes by 20 THz infrared laser pulses in X-ray diffraction pump-probe experiments [28] have indicated a pico-second short transient superconducting state above room-temperature in YBCO. The Cu(1)-O(4) stretching mode (A_g symmetry) couples to the transverse mode (B_{1u} symmetry) [29] of the apical oxygen atoms between the planes and the chains that is involved in the self-doping process.

3.3. *O* 1s*-edge XAS*

The O *1s* edge XAS and O *K* RIXS spectra of YBCO give additional clues about the nature and temperature dependence of the elec-

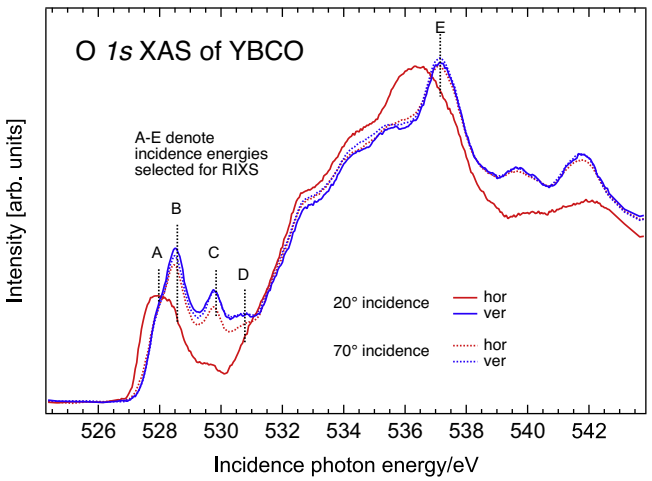

Fig. 5. O *K* XAS of optimally doped YBCO for two different incident polarizations and two different incidence angles.

tronic structure of high temperature superconductors. Previously, using O *1s* XAS, Merz *et al.* [30] estimated the hole distribution for $x = 6.91$ in the CuO_2 plane, at the apical O and in the Cu-O chain as 0.40, 0.27 and 0.24, respectively. Fig. 5 displays high resolution polarization dependent O *1s*-XAS for optimally doped YBCO [31]. The crystal anisotropy (**E**||**c** vs **E**||**ab**) is clearly reflected by the polarization differences in the O*1s*-edge spectra as well as at the Cu *2p*-edge. Horizontally and vertically polarized synchrotron radiation was used for two different incidence angles, 20° and 70°. For vertical polarization, the polarization vector of the incident X-rays **E**, is parallel to the CuO_2-planes, independent of the incidence angle. For the horizontal polarization, the polarization vector of the incident X-rays is dominantly in plane (out of plane) for 70° (20°), relative to the sample surface plane. This means that the polarization vector only has a significant out of plane component in the configuration of horizontal polarization at an incidence angle of 20° relative to the surface plane. This is observed in Fig. 5 as the solid red trace that is significantly different from the other three traces for which the polarization vector is almost in plane. The pre-peak region, where the O *1s* electron is excited into the (doping-induced) Zhang-Rice [3] band (ZRB) and the upper Hubbard band (UHB), respectively, is of main interest since these states involve hybridization with the correlated Cu *3d*-orbitals. The UHB (denoted C in Fig. 5) is highly polarized in plane, while there is additional intensity on the low energy shoulder of ZRB (A and B in Fig. 5) when the incident polarization vector is almost parallel with (the out of plane) the crystal axis *c*. This feature (A), corresponds to the Cu(1)-O(4) apical oxygen and chain excitations [31].

3.4. *O* K-*edge RIXS*

Fig. 6 displays polarization dependent RIXS spectra (using 70 meV combined resolution) with incident energies in the region of the ZRB and the UHB. We observe a main band (525–527 eV) with a low-energy shoulder (522–525 eV) nearly stationary in photon energy that we can assign to O *2p*-states that are more or less covalently hybridized with Cu *3d*-orbitals, depending on the excitation energy. This state consists of *dd*-excitations that show a strong polarization dependence at the lowest incident energy (A) [32,33], corresponding to the inequivalent O(4) apical oxygen and O(1) chain sites. Previous O *K* RIXS studies with **E**||**ab** suggested that O(2,3) with $x = 6.94$ have higher binding energy than those of O(1) and O(4) [34]. At 20° incidence, the main O *2p* peak is more localized at 526.2 eV emission energy, which is not enhanced by self-absorption effects [15] because these are less significant than

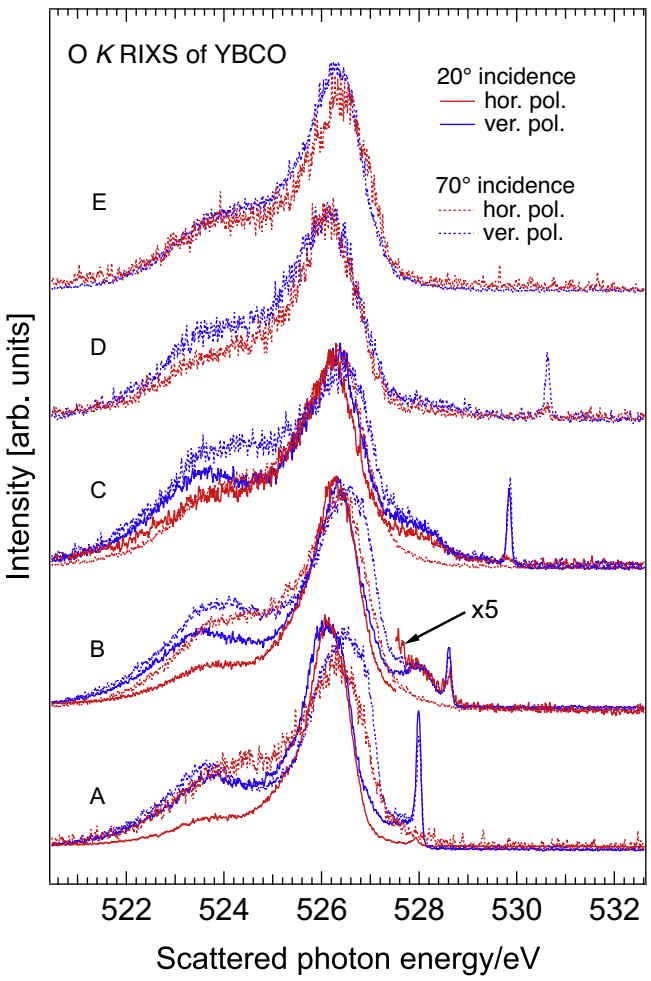

Fig. 6. Polarization dependent RIXS excited with incident energies (denoted A-E) as depicted in Fig. 4.

at 70° incidence angle. Furthermore, an interesting feature resonating at the ZRB peak B is observed to be strongly enhanced in vertical polarization, i.e. σ-scattering, both for the 20°- and the 70°-incidence angle. This feature, which has a loss energy of less than 1 eV, does not show any significant temperature dependence. This observation is reminiscent of the bimagnons observed in O *K* RIXS for e.g. of $La_xSr_{1-x}CuO_4$ observed by Bisogni *et al.* [35], apart from the higher energy loss excitation of more than 0.5 eV that we record for YBCO.

For horizontal incidence polarization, *i.e.* π-scattering, no ZRB RIXS feature appears for (nearly) in-plane (**E**||**ab**) polarization, *i.e.* at a 70° incidence angle of the X-rays on the sample (red dashed trace). Interestingly, at a 20° incidence angle (red solid trace) there is a small contribution. The ratio between the oxygen main band and the ZRB RIXS feature is about 5 times as large as for vertical polarization (we therefore provide a blow-up of this part of the spectrum in Fig. 6 with a corresponding scaling factor, see arrow). This observation emphasizes the completely different origins of these two spectral features. It is likely due to the two-dimensional character of the involved orbitals that prevents the suppression of intensity in this geometry for the oxygen main band feature.

We now turn to the discussion of the possible origin of the ZRB RIXS feature. From Cu *L* RIXS (Fig. 2) we know that the single magnon has an energy around 0.2 eV, so that bimagnons are allowed to appear at most at about double the energy, *i.e.* ∼0.4 eV. We have also investigated the doping dependence of these excitations and plotted the result in Fig. 7. Note that there is a shift to

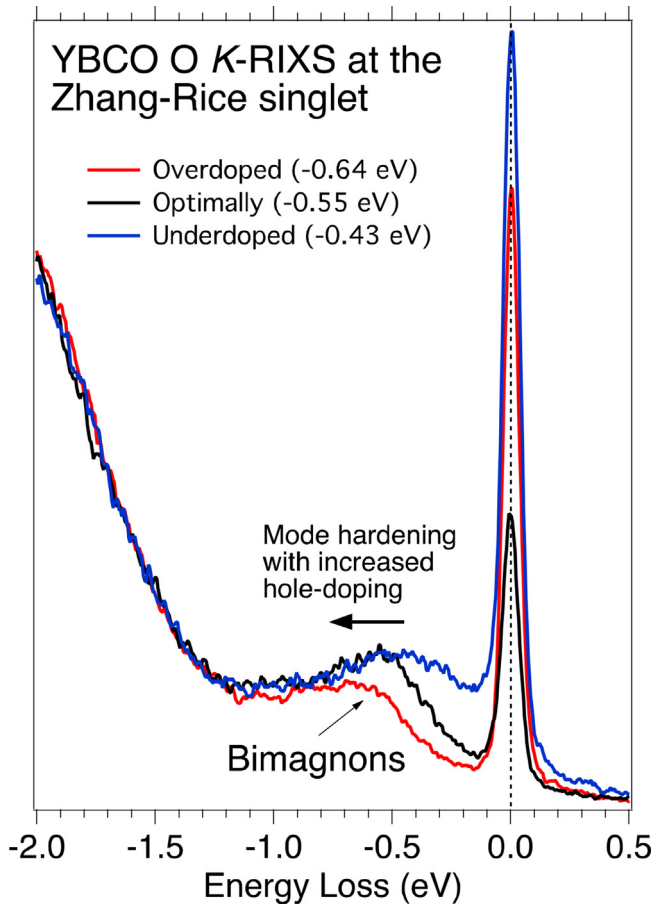

Fig. 7. Doping dependent O *K*-RIXS that shows how the collective excitations harden for higher oxygen doping levels.

higher loss energy (*i.e.* a *hardening*) with increasing oxygen doping, which is unexpected if it were an ordinary bimagnon excitation [35,36]. The hardening of this mode as doping increases is *opposite* to the behavior of the magnetic excitation spectra observed at the Cu *L*-resonance of the YBCO system [16]. Also at the Cu *K* and *L*-edges magnons are found to shift towards lower energy with increasing hole doping. For the LaSrCuO-system, one has only found rather little *q*-dependence [35], which was rationalized as being the effect of momentum averaging and thus reflecting the high-energy density of magnon states. For YBCO, a *q*-dependence has not yet been reported for bimagnons so far but we have preliminary indications that this feature also has a momentum dependent sine-shaped behavior. The recent discovery of a strongly dispersive high energy mode by Ishii *et al.* [17] has been attributed to charge excitations with a parabolic-shaped dispersion. Contrary to magnon dispersion, charge-excitations are not limited in excitation-energy and low-energy orbital excitations might involve both Cu and O in the chains. Our finding of a relatively intense spectral feature in the mid IR region is indeed peculiar to YBCO, as LSCO and the quasi 1D cuprates do not show any intensity in that energy range. The doping-dependence is also puzzling with hardening of the excitation with increasing hole doping. However, the dispersion behaviors are markedly distinct and for YBCO the momentum dependent behavior is AFM-like [39]. Recently Lee *et al.* [37] resolved site-dependent low-energy excitations arising from progressive emissions of a 70 meV lattice vibrational mode in $Ca_{2+5x}Y_{2-5x}Cu_5O_{10}$. The dispersion of bimagnons are not yet fully understood and only some guiding theory exists [38]. We tentatively assign these excitations to collective magnetic excitations within the ZR and/or the Hubbard bands. However, further work is needed to assign this feature more definitely, as the assignment to complex collective magnetic excitations is not well understood theoretically. A forthcoming publication will discuss these excitations in more depth [39].

4. Summary and conclusions

To summarize, we present high resolution XAS and RIXS results at the Cu *L* and the O *K* edges of $YBa_2Cu_3O_{6.9}$. Ligand-field multiplet calculations describe the observed *dd*-excitations very well and a spin flip excitation is found to be consistent with Cu *L* RIXS at medium momentum transfer. A novel doping and incident energy-dependent feature at around 0.5–0.6 eV is observed in O *K* RIXS of YBCO. This ZRB RIXS feature is interpreted as a bimagnon excitation within the Zhang-Rice and/or Hubbard bands of YBCO. No temperature dependence could be observed for this mode, which suggests that it might not be directly involved in the MST. It is large for π-scattering (vertical polarization). On the other hand, for σ-scattering (horizontal polarization) it is much smaller for grazing incidence (20°) and completely absent for grazing exit (70°). Intriguingly, the mode hardens unexpectedly with oxygen doping.

Acknowledgements

The experiments have been carried out at the ADRESS beamline of the Swiss Light Source (SLS) at the Paul Scherrer Institut and we would like to thank the staff at the SLS for experimental support. We acknowledge A. S. Kalabukhov for providing the thin film samples and F de Groot for fruitful discussions. This work was supported by the Swedish Research Council (VR) Linnaeus Grant LiLi-NFM, the FUNCASE project (no. RMA11-0029) by the Swedish Strategic Research Foundation (SSF). MM acknowledges financial support from the Swedish Energy Research (no. 43606-1) and the Carl Tryggers Foundation (CTS16:303, CTS14:310).

References

[1] The rise of the superconductors, in: P.J. Ford (Ed.), The Rise of the Superconductors, CRC Press, 2005 (2005).
[2] J. Bardeen, L.N. Cooper, J.R. Schrieffer, Theory of superconductivity, Phys. Rev. 108 (1957) 1175–1204.
[3] F.C. Zhang, T.M. Rice, Effective Hamiltonian for the superconducting Cu oxides, Phys. Rev. B 37 (1988) 3759 (R).
[4] M. Magnuson, T. Schmitt, V.N. Strocov, J. Schlappa, A.S. Kalabukhov, Self-doping processes between planes and chains in the metal-to-superconductor transition of $YBa_2Cu_3O_{6.9}$, Sci. Rep. 4 (2014) 7017.
[5] G. Ghiringhelli, A. Piazzalunga, C. Dallera, G. Trezzi, L. Braicovich, T. Schmitt, V.N. Strocov, R. Betemps, L. Patthey, X. Wang, M. Grioni, SAXES, a high resolution spectrometer for resonant x-ray emission in the 400–1600 eV energy range, Rev. Sci. Instrum. 77 (2006) 113108.
[6] V.N. Strocov, T. Schmitt, U. Flechsig, T. Schmidt, A. Imhof, Q. Chen, J. Raabe, R. Betemps, D. Zimoch, J. Krempasky, X. Wang, M. Grioni, A. Piazzalunga, L. Patthey, High-resolution soft X-ray beamline ADRESS at the Swiss light source for resonant inelastic X-ray scattering and angle-resolved photoelectron spectroscopies, J. Synchr. Radiat. 17 (2010) 631.
[7] G. Ghiringhelli, L. Braicovich, T. Schmitt, V. Strocov, High-resolution RIXS with the SAXES spectrometer at the ADRESS beamline of the swiss light source, Synchrotron Rad. News. 25 (4) (2012) 16–22.
[8] H.A. Kramers, W. Heisenberg, Über die Streuung von Strahlung durch Atome, Z. Phys. 31 (1925) 681.
[9] R.D. Cowan, The Theory of Atomic Structure and Spectra, University of California Press, Berkeley, CA, 1981 (Berkeley, CA: University of California Press, 1981).
[10] M. Magnuson, S.M. Butorin, J.-H. Guo, J. Nordgren, Electronic structure investigation of CoO by means of soft X-ray scattering, Phys. Rev. B 65 (2002) 205106.
[11] M. Magnuson, S.M. Butorin, A. Agui, J. Nordgren, Resonant soft X-ray Raman scattering of NiO, J. Phys. Condens. Matter 14 (2002) 3669.
[12] P.W. Anderson, Localized magnetic states in metals, Phys. Rev. B 124 (1961) 41.
[13] P.H. Butler, Point Group Symmetry Applications: Methods and Tables, Plenum, New York, 1981 (New York: Plenum, 1981).
[14] F. de Groot, A. Kotani, Core Level Spectroscopy of Solids, CRC Press, 2008 (CRC Press, 2008).

[15] M. Magnuson, N. Wassdahl, J. Nordgren, Energy dependence of Cu $L_{2,3}$ satellite structures using synchrotron excited X-ray emission spectroscopy, Phys. Rev. B 56 (1997) 12238.
[16] M. Le Tacon, G. Ghiringhelli, J. Chaloupka, M. Moretti Sala, V. Hinkov, M.W. Haverkort, M. Minola, M. Bakr, K.J. Zhou, S. Blanco-Canosa, C. Monney, Y.T. Song, G.L. Sun, C.T. Lin, G.M. De Luca, M. Salluzzo, G. Khaliullin, T. Schmitt, L. Braicovich, B. Keimer, Intense paramagnon excitations in a large family of high- temperature superconductors, Nat. Phys. 7 (2011) 725.
[17] K. Ishii, M. Fujita, T. Sasaki, M. Minola, G. Dellea, C. Mazzoli, K. Kummer, G. Ghiringhelli, L. Braicovich, T. Tohyama, K. Tsutsumi, K. Sato, R. Kajimoto, K. Ikeuchi, K. Yamada, M. Yoshida, M. Kurooka, J. Mizuki, High-energy spin and charge excitations in electron-doped copper oxide superconductors, Nat. Commun. 5 (2014) 3714.
[18] L. Braicovich, J. van den Brink, V. Bisogni, M. Moretti Sala, L.J.P. Ament, N.B. Brookes, G.M. De Luca, M. Salluzzo, T. Schmitt, V.N. Strocov, G. Ghiringhelli, Magnetic Excitations and Phase Separation in the Underdoped $La_{2-x}Sr_xCuO_4$ Superconductor Measured by Resonant Inelastic X-Ray Scattering, Phys. Rev. Lett. 104 (2010) 077002.
[19] M.P.M. Dean, A.J.A. James, R.S. Springell, X. Liu, C. Monney, K.J. Zhou, R.M. Konik, J.S. Wen, Z.J. Xu, G.D. Gu, V.N. Strocov, T. Schmit, J.P. Hill, High-energy magnetic excitations in the cuprate superconductor $Bi_2Sr_2CaCu_2O_{8+\delta}$: towards a unified description of its electronic and magnetic degrees of freedom, Phys. Rev. Lett. 110 (2013) 147001.
[20] J. Schlappa, T. Schmitt, F. Vernay, V.N. Strocov, V. Ilakovac, B. Thielemann, H.M. Rønnow, S. Vanishri, A. Piazzalunga, X. Wang, L. Braicovich, G. Ghiringhelli, C. Marin, J. Mesot, B. Delley, L. Patthey, Collective magnetic excitations in the spin ladder $Sr_{14}Cu_{24}O_{41}$ measured using high-resolution resonant inelastic X-ray scattering, Phys. Rev. Lett. 103 (2009) 047401.
[21] M. Magnuson, L.-C. Duda, S.M. Butorin, P. Kuiper, J. Nordgren, Large magnetic circular dichroism in resonant inelastic x-ray scattering at the Mn *L*-edge of Mn-Zn ferrite, Phys. Rev. B 74 (2006) 172409.
[22] D. Perry, Applications of Analytical Techniques to the Characterization of Materials, Springer Science & Business Media, 1991.
[23] G. Ghiringhelli, M. Le Tacon, M. Minola, S. Blanco-Canosa, C. Mazzoli, N.B. Brookes, G.M. De Luca, A. Frano, D.G. Hawthorn, F. He, T. Loew, M. Moretti Sala, D.C. Peets, M. Salluzzo, E. Schierle, R. Sutarto, G.A. Sawatzky, E. Weschke, B. Keimer, L. Braicovich, Long-range incommensurate charge fluctuations in $(Y,Nd)Ba_2Cu_3O_{6-x}$, Science 337 (2012) 821.
[24] V.B. Zabolotnyy, A.A. Kordyuk, D. Evtushinsky, V.N. Strocov, L. Patthey, T. Schmitt, D. Haug, C.T. Lin, V. Hinkov, B. Keimer, B. Büchner, S.V. Borisenko, Pseudogap in the chain states of $YBa_2Cu_3O_{6.6}$, Phys. Rev. B 85 (2012) 064507.
[25] J. Schlappa, K. Wohlfeld, K.J. Zhou, M. Mourigal, M.W. Haverkort, V.N. Strocov, L. Hozoi, C. Monney, S. Nishimoto, S. Singh, A. Revcolevschi, J.-S. Caux, L. Patthey, H.M. Rønnow, J. van den Brink, T. Schmitt, Spin-orbital separation in the quasi-one-dimensional Mott insulator Sr_2CuO_3, Nature 82 (2012).
[26] J. Igarashi, T. Nagao, Magnetic excitations in L-edge resonant inelastic x-ray scattering from cuprate compounds, Phys. Rev. B 85 (2012) 064421.
[27] C. Luo, T. Datta, D.-X. Yao, Spectrum splitting of bimagnon excitations in a spatially frustrated Heisenberg antiferromagnet revealed by resonant inelastic x-ray scattering, Phys. Rev. B 89 (2014) 165103.
[28] R. Mankowsky, A. Subedi, M. Först, S.O. Mariager, M. Chollet, H.T. Lemke, J.S. Robinson, J.M. Glownia, M.P. Minitti, A. Frano, M. Fechner, N.A. Spaldin, T. Loew, B. Keimer, A. Georges, A. Cavalleri, Nonlinear lattice dynamics as a basis for enhanced superconductivity in $YBa_2Cu_3O_{6.5}$, Nature 516 (2014) 71–73.
[29] R. Mankowsky, M. Först, A. Cavalleri, Non-equilibrium control of complex solids by nonlinear phononics, Rep. Prog. Phys. 79 (2016) 064503.
[30] M. Merz, N. Nücker, P. Schweiss, S. Schuppler, C.T. Chen, V. Chakarian, J. Freeland, J.U. Idzerda, M. Kläser, G. Müller-Vogt, T. Wolf, Site-specific X-ray absorption spectroscopy of $Y_{1-x}Ca_xBa_2Cu_3O_{7-y:}$ overdoping and role of apical oxygen for high temperature superconductivity, Phys. Rev. Lett. 80 (1998) 5192.
[31] N. Nücker, E. Pellegrin, P. Schweiss, J. Fink, S.L. Molodtsov, C.T. Simmons, G. Kaindl, W. Frentrup, A. Erb, G. Müller-Vogt, Site-specific and doping-dependent electronic structure of $YBa_2Cu_3O_x$ probed by O *1 s* and Cu *2p* x-ray-absorption spectroscopy, Phys. Rev. B 51 (1995) 8529.
[32] M.A. Hossain, J.D.F. Mottershead, D. Fournier, A. Bostwick, J.L. McChesney, E. Rotenberg, R. Liang, W.N. Hardy, G.A. Sawatzky, I.S. Elfimov, D.A. Bonn, A. Damascelli, In situ doping control of the surface of high-temperature superconductors, Nat. Phys. 4 (2008) 527.
[33] L.-C. Duda, J. Downes, C. McGuinness, T. Schmitt, A. Augustsson, K.E. Smith, G. Dhalenne, A. Revcolevschi, Bandlike and excitonic states of oxygen in $CuGeO_3$: observation using polarized resonant soft-x-ray emission spectroscopy, Phys. Rev. B 61 (2000) 4186.
[34] J.-H. Guo, S.M. Butorin, N. Wassdahl, J. Nordgren, P. Berastegut, L.-G. Johansson, Electronic structure of $YBa_2Cu_3O_x$ and $YBa_2Cu_4O_8$ studied by soft-x-ray absorption and emission spectroscopies, Phys. Rev. B 61 (2000) 9140.
[35] V. Bisogni, L. Simonelli, L.J.P. Ament, F. Forte, M. Moretti Sala, M. Minola, S. Huotari, J. van den Brink, G. Ghiringhelli, N.B. Brookes, L. Braicovich, Bimagnon studies in cuprates with resonant inelastic x-ray scattering at the O K edge. I. Assessment on La_2CuO_4 and comparison with the excitation at Cu L_3 and Cu K edges, Phys. Rev. B 85 (2012) 214527, ibid. 85, 214528 (2012).
[36] D.S. Ellis, J. Kim, H. Zhang, J.P. Hill, G. Gu, S. Komiya, Y. Ando, D. Casa, T. Gog, Y.-J. Kim, Electronic structure of doped lanthanum cuprates studied with resonant inelastic x-ray scattering, Phys. Rev. B 83 (2011) 075120.
[37] W.S. Lee, S. Johnston, B. Moritz, J. Lee, M. Yi, K.J. Zhou, T. Schmitt, L. Patthey, V. Strocov, K. Kudo, Y. Koike, J. van den Brink, T.P. Devereaux, Z.X. Shen, Role of lattice coupling in establishing electronic and magnetic properties in quasi-one-dimensional cuprates, Phys. Rev. Lett. 110 (2013) 265502.
[38] F. Forte, M. Cuoco, C. Noce, J. van den Brink, Doping dependence of magnetic excitations of one-dimensional cuprates as probed by resonant inelastic x-ray scattering, Phys. Rev. B 83 (2011) 245133.
[39] M. Magnuson, T. Schmitt, A.S. Kalabukhov, L.-C. Duda, Coherent Bimagnon Excitations Observed in $YBa_2Cu_3O_{7-x}$, 2017 (in manuscript).